The electric field in capacitively coupled RF discharges: a smooth step model that includes thermal and dynamic effects

2015 Plasma Sources Sci. Technol. 24 064002

(http://iopscience.iop.org/0963-0252/24/6/064002)

IOP Publishing Plasma Sources Science and Technology

Plasma Sources Sci. Technol. **24** (2015) 064002 (16pp) doi:10.1088/0963-0252/24/6/064002

The electric field in capacitively coupled RF discharges: a smooth step model that includes thermal and dynamic effects

Ralf Peter Brinkmann

Institute for Theoretical Electrical Engineering, Research Department Plasmas with Complex Interactions
Ruhr University Bochum, D-44780 Bochum, Germany

E-mail: Ralf-Peter.Brinkmann@tet.rub.de

Received 17 March 2015, revised 3 June 2015
Accepted for publication 16 June 2015
Published 8 October 2015

Abstract

The electric field in radio-frequency driven capacitively coupled plasmas (RF-CCP) is studied, taking thermal (finite electron temperature) and dynamic (finite electron mass) effects into account. Two dimensionless numbers are introduced, the ratios $\epsilon = \lambda_D/l$ of the electron Debye length λ_D to the minimum plasma gradient length l (typically the sheath thickness) and $\eta = \omega_{RF}/\omega_{pe}$ of the RF frequency ω_{RF} to the electron plasma frequency ω_{pe}. Assuming both numbers small but finite, an asymptotic expansion of an electron fluid model is carried out up to quadratic order inclusively. An expression for the electric field is obtained which yields (i) the space charge field in the sheath, (ii) the generalized Ohmic and ambipolar field in the plasma, and (iii) a smooth interpolation for the transition in between. The new expression is a direct generalization of the *Advanced Algebraic Approximation (AAA)* proposed by the same author (2009 *J. Phys. D: Appl. Phys.* **42** 194009), which can be recovered for $\eta \to 0$, and of the established *Step Model (SM)* by Godyak (1976 *Sov. J. Plasma Phys.* **2** 78), which corresponds to the simultaneous limits $\eta \to 0$, $\epsilon \to 0$. A comparison of the hereby proposed *Smooth Step Model (SSM)* with a numerical solution of the full dynamic problem proves very satisfactory.

Keywords: plasma boundary sheath, electrical field, capacitively coupled plasma

(Some figures may appear in colour only in the online journal)

1. Introduction

For several decades now, radio frequency capacitively coupled plasmas (RF-CCPs) are the workhorses of plasma technology [1]. Nonetheless, many of the complex physical mechanisms that underlie their operation are not yet fully understood. This holds particularly for the subject of this Special Issue, the various electron heating mechanisms and the resulting electron energy distribution functions (EEDFs). Recent research has revealed many unexpected and interesting details, and it is no exeggaration to state that the traditional understanding of electron heating has proved inadequate [2–4]. A new paradigm, however, is slow to emerge. This work aims to contribute by analyzing a quantity central to electron heating in RF-CCPs, namely the temporally and spatially structured electrical field.

Fundamentally, of course, all electromagnetic fields are given, via Maxwell's equations, by the distribution of electric charges and currents. In a plasma, however, where the charges and currents in turn are governed by the electromagnetic fields, Maxwell's equations are coupled to the electron and ion transport equations which thus must be solved simultaneously. The arising self-consistency problem is notoriously difficult, even under the so-called electrostatic approximation which reduces Maxwell's equations to the simpler Poisson equation. Of course, one may approach the problem numerically, for example by simulation techniques such as particle-in-cell Monte Carlo (PIC-MC), but these methods are computationally costly and their interpretation is often problematic without commanding analytical insight.

In this situation, techniques are of interest which reduce the mathematical complexity of a plasma model under study

but preserve the essence of its physics. This work is concerned with a particular class of plasmas, namely capacitive discharges, and focuses on a particular class of simplifications, namely those which replace the electron momentum balance and the Poisson equation—a system of coupled differential equations—with an algebraic formula, i.e. with a closed expression that contains no differential equations to be solved.

The pioneering algebraic field formula is the *Step Model (SM)* by Godyak [5]. Observing that in a plasma-sheath transition the passage from quasineutrality to full electron depletion is quite steep, Godyak modeled the electron density by an infinitely sharp front (step) located at the electron sheath edge $s(t)$. Poisson's equation then resulted in an explicit formula for the electric field which correctly captures the space charge field in the electron depleted sheath and represents the (much weaker) plasma field as zero.

The Step Model has found many applications, notably in the two early RF sheath models by Lieberman [6, 7] and later generalizations [8–14]. It has one essential weakness, though: It gives the electric field only in the sheath, not in the plasma, and thus forces to postulate (somewhat problematic) boundary conditions at the (decidedly problematic) 'sheath edge'. To correct this deficiency, this author recently proposed an alternative field model based on an asymptotic solution of Poisson's equation and the electron equilibrium condition [15, 16]:

The *Advanced Algebraic Approximation* (AAA) establishes an algebraic expression for the electric field in a plasma-sheath transition which (i) yields the space charge field in the electron depleted sheath, (ii) reduces to the ambipolar field in the quasineutral plasma, and (iii) provides a resonable nonlinear interpolation in between. As the appellation implies, the AAA is also an approximation; it was derived under the assumption that the local Debye length $\lambda_D = \sqrt{\epsilon_0 T_e/e^2 n_i}$ is small compared to the local ion density scale length $l = n_i/\frac{\partial n_i}{\partial x}$. The AAA can thus be seen as an improved version of the SM: Instead of simply assuming a sharp electron edge which separates the zones of electron depletion and quasineutrality, thermal corrections are systematically accounted for up to quadratic order in $\epsilon = \lambda_D/l \ll 1$. The AAA was sucessfully employed for the modeling of DC and RF plasma boundary sheaths and provided also a new view on the collisionally modified Bohm criterion [17–20].

For the investigation of this PSST Special Issue's subject, however, the AAA is not suited: The underlying assumption of exact force equilibrium makes the AAA ignore the dynamic and dissipative contributions to the electric field. Heating (irreversible energy transfer from the field to the electrons) can thus not be captured. In addition, the electron temperature T_e is described as a given constant—also incompatible with the process of heating [2, 10]. This study will amend the Step Model even further and bring it, in a way, into its final form: Including electron inertia and collisions and allowing for a variable electron temperature, the *Smooth Step Model (SSM)* will be stated that yields (i) the space charge field in the sheath, (ii) the generalized Ohmic field in the plasma, and (iii) a smooth interpolation in between. For this purpose, the assumption of *exact* force equilibrium will be dropped and replaced by the assumption of *approximate* force equilibrium where the small differential represents the forces of electron inertia and collisions. The RF frequency ω_{RF} and the collision frequency ν_{ce} are assumed to be small compared to the plasma frequency ω_{pe}, and a second smallness parameter $\eta = \omega_{RF}/\omega_{pe} \sim \nu_{ce}/\omega_{pe} \ll 1$ is invoked in addition to ϵ. In the final field formula, correction terms up to quadratic order in both η or ϵ will be kept.

For illustration purposes, table 1 lists the characteristic quantities of two argon discharges at $p = 2\,\mathrm{Pa}$ and $T_n = 300\,\mathrm{K}$, driven at $f_{RF,I} = 13.56\,\mathrm{MHz}$ and $f_{RF,II} = 67.8\,\mathrm{MHz}$, respectively. The given scales can be used to translate the dimensionless results of figures 1–8 back into physical units. Note that the presented arguments do not rely on any numerical details but only on the smallness of the numbers ϵ and η.

2. Electron equilibrium model

This research aims to study the electrical field in capacitively coupled plasmas under conditions where the electrons are not in exact force equilibrium. For later comparison, however, it is useful to first review the algebraic models SM and AAA that make that assumption. Note that the models do *not* assume a static state. Instead, the equilibrium is parametrically modulated by the RF current density $\tilde{j}(t)$ which is a given average-free quantity.

Both SM and AAA stem from the same ancestor, the *Electron Equilibrium Model (EQ)*. A planar geometry is assumed where the x-axis points from the electrode x_E to the plasma. (The origin $x = 0$ is not located at x_E but rather at the point $\bar{s}$ which will be defined below.) A suitable point x_B in the plasma is fixed so that the physical solution domain is $[x_E, x_B]$. It is mathematically convenient to formally extend the solution domain to the full real axis; the 'virtual' regions left of x_E and right of x_B allow to employ a set of transparent asymptotic conditions instead of problematic boundary conditions. (See figure 1.)

The ion density $n_i(x)$ is prescribed as a continuous, monotonically growing function of x. It is not RF modulated, on grounds that the applied radio frequency ω_{RF} is much larger than the ion plasma frequency ω_{pi}. (The error introduced by this assumption scales with $\omega_{pi}^2/\omega_{RF}^2$.) The electron density $n_e(x,t)$ follows the condition of exact force (or Boltzmann) equilibrium which implies that, for any given time, the electric force is balanced by the pressure force. For a constant electron temperature T_e this reads

$$T_e \frac{\partial n_e}{\partial x} + e n_e E = 0. \tag{1}$$

Poisson's equation relates the difference of the ion and electron charge densities to the phase-resolved electrical field $E(x,t)$,

Table 1. Characteristic scales and dimensionless numbers for two RF CCP examples.

Unit	Symbol	Definition	Example I	Example II
Modulation frequency	ω_{RF}	Assumed	$8.52\times10^{7}\,s^{-1}$	$4.26\times10^{8}\,s^{-1}$
Time scale	T	$1/\omega_{RF}$	$1.17\times10^{-8}\,s$	$2.35\times10^{-9}\,s$
Voltage scale	$\hat{V}$	Assumed	300 V	300 V
Ion flux	ψ_i	Assumed	$2\times10^{19}\,m^{-2}\,s^{-1}$	$2\times10^{19}\,m^{-2}\,s^{-1}$
Density scale	$\hat{n}$	$\sqrt{m_i\psi_i^2/e\hat{V}}$	$7.43\times10^{14}\,m^{-3}$	$7.43\times10^{14}\,m^{-3}$
Length scale	l	$\sqrt[4]{\epsilon_0^2\hat{V}^3/em_i\psi_i^2}$	$4.72\times10^{-3}\,m$	$4.72\times10^{-3}\,m$
RF current scale		$e\hat{n}\omega_{RF}l$	$47.9\,A/m^2$	$240\,A\,m^{-2}$
Electron speed scale		l/T	$4.02\times10^{5}\,m\,s^{-1}$	$2.01\times10^{6}\,m\,s^{-1}$
Ion speed scale		$\sqrt{e\hat{V}/m_i}$	$2.69\times10^{4}\,m\,s^{-1}$	$2.69\times10^{4}\,m\,s^{-1}$
Electron temperature scale	$\hat{T}_e$	Assumed	3 eV	3 eV
Debye length	λ_D	$\sqrt{\epsilon_0\hat{T}_e/e^2\hat{n}}$	$4.72\times10^{-4}\,m$	$4.72\times10^{-4}\,m$
Electron plasma frequency	ω_{pe}	$\sqrt{e^2\hat{n}/\epsilon_0m_e}$	$1.54\times10^{9}\,s^{-1}$	$1.54\times10^{9}\,s^{-1}$
Ion plasma frequency	ω_{pi}	$\sqrt{e^2\hat{n}/\epsilon_0m_i}$	$5.69\times10^{6}\,s^{-1}$	$5.69\times10^{6}\,s^{-1}$
Neutral gas density	n_n	Assumed	$4.83\times10^{20}\,m^{-3}$	$4.83\times10^{20}\,m^{-3}$
Transition speed	v_T	Assumed	$630\,m\,s^{-1}$	$630\,m\,s^{-1}$
Ion mean free path	λ_i	Assumed	$1.94\times10^{-3}\,m$	$1.94\times10^{-3}\,m$
Electron collision frequency	ν_{ce}	Assumed	$4.83\times10^{7}\,s^{-1}$	$4.83\times10^{7}\,s^{-1}$
Length scale ratio	ϵ	λ_D/l	0.1	0.1
Frequency ratio	η	ω_{RF}/ω_{pe}	0.0554	0.277
Scaled transition speed	u_T	$v_T/\sqrt{e\hat{V}/m_i}$	0.0234	0.0234
Scaled ion mean free path	λ	λ_i/l	0.410	0.410
Scaled electron collision frequency	ν	ν_{ce}/ω_{RF}	0.567	0.113
Scaled RF current	$\tilde{j}$	$\tilde{j}/e\hat{n}\omega_{RF}l$	$\sin(t)$	$\sin(t)$
Scaled applied bias voltage	$\bar{V}$	$\bar{V}/\hat{V}$	1	1

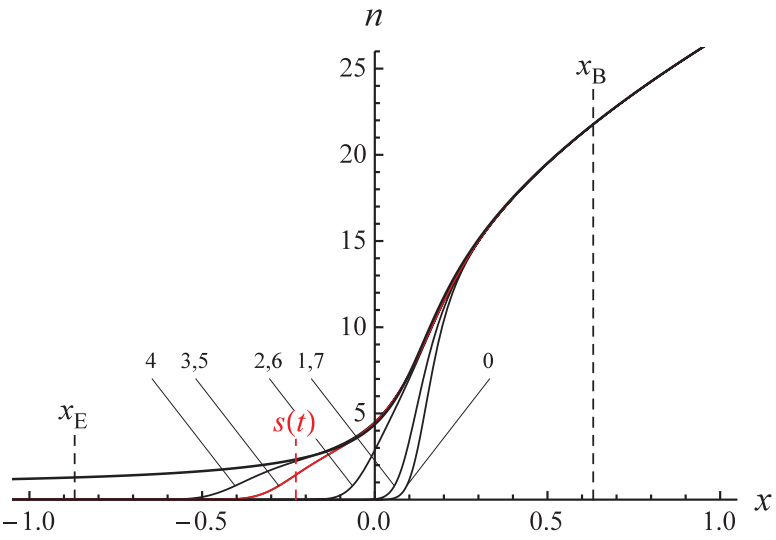

Figure 1. Phase-resolved electron and ion densities in an RF modulated sheath-plasma transition, calculated with the Electron Equilibrium Model (EQ) and the ion model described in section IV. The x-axis points from the electrode x_E into the plasma, where a point x_B is chosen as reference. For mathematical convenience, the physical solution domain $[x_E, x_B]$ is extended to the full real axis by means of the virtual regions $x < x_E$ and $x > x_B$. Note that the coordinate origin $x = 0$ is located not at x_E but at the point $\bar{s}$ defined in the text. The ion density $n_{i,EQ}(x)$ (thick) is stationary; the electron density $n_{e,EQ}(x,t)$ (thin) is modulated, shown here at the times $t_k = k\pi/4$, $k = 0..7$. (Because of the symmetry $t \to 2\pi - t$, the curves of the expanding and retracting phase conincide.) The red line highlights $n_{e,EQ}(x,t)$ and the corresponding electron sheath edge $s(t)$ at $t_3 = 3\pi/4$.

$$\epsilon_0 \frac{\partial E}{\partial x} = e(n_\mathrm{i} - n_\mathrm{e}). \tag{2}$$

The system of (1) and (2) contains two degrees of freedom. One constraint is the condition of quasineutrality and vanishing field strength for $x \gg x_\mathrm{B}$; together with the assumption of electron depletion for $x \ll x_\mathrm{E}$ this ensures sheath-like solutions as depicted in figure 1,

$$n_\mathrm{e}(x,t) \underset{x \gg x_\mathrm{B}}{\longrightarrow} n_\mathrm{i}(x), \tag{3}$$

$$E(x,t) \underset{x \gg x_\mathrm{B}}{\longrightarrow} 0, \tag{4}$$

$$n_\mathrm{e}(x,t) \underset{x \ll x_\mathrm{E}}{\longrightarrow} 0. \tag{5}$$

The second degree of freedom describes the actual location of the transition from electron depletion to quasineutrality. It is convenient to borrow, in modified form, the central concept of the Step Model: For a given set of ion and electron densities, the *electron sheath edge* s is formally defined as the point where the total electron charge to the left equals the 'missing' electron charge to the right [15, 22],

$$\Delta := \int_{-\infty}^{s} e n_\mathrm{e}\,\mathrm{d}x - \int_{s}^{\infty} e(n_\mathrm{i} - n_\mathrm{e})\,\mathrm{d}x \stackrel{!}{=} 0. \tag{6}$$

Note that this implicit definition of s is consistent, as equation (6) has a unique solution: Seen as a function of s, the quantity Δ grows continuously and monotonically from $-\infty$ to ∞, so that the existence and uniqueness of its zero s is guaranteed. The inverse is also true: For any given value of s, there is a unique solution of the Boltzmann-Poisson system [15]. The location of the electron sheath edge thus fixes the second degree of freedom.

Of course, under RF modulation, an electron flux $\psi_\mathrm{e}(x,t)$ is present and the electron density and the electron sheath edge vary in time. Assuming that ionization and attachment can be neglected as relatively slow processes, the electron equation of continuity states

$$\frac{\partial n_\mathrm{e}}{\partial t} + \frac{\partial \psi_\mathrm{e}}{\partial x} = 0. \tag{7}$$

Taking the time derivative of Poisson's equation (2), using (7), and integrating from $-\infty$ to x, one finds that the sum of the electron current and the displacement current is a spatial constant which, because of the asymptotic conditions, can be identified with the RF current. The ion contribution can be neglected as $\omega_\mathrm{pi} \ll \omega_\mathrm{RF}$,

$$-e\psi_\mathrm{e} + \epsilon_0 \frac{\partial E}{\partial t} = \tilde{j}\,(t). \tag{8}$$

The average-free negative integral of $\tilde{j}\,(t)$ is introduced as the fluctuating sheath charge

$$\tilde{Q}(t) = -\int_0^t j(t')\,\mathrm{d}t' + \int_0^T \left(1 - \frac{t'}{T}\right) j(t')\,\mathrm{d}t'. \tag{9}$$

Now consider the quantity Δ as a function of time t via the electron sheath edge $s(t)$ and the electron density $n_\mathrm{e}(x,t)$. Numerically, of course, it vanishes, but the partial differential derivative with respect to t can be taken nonetheless. Invoking the equation of continuity, it turns out that $s(t)$ follows the definition of the electron sheath edge (see, e.g. [6]),

$$\begin{aligned} e n_\mathrm{i}(s(t)) \frac{\mathrm{d}s}{\mathrm{d}t} &= -\int_{-\infty}^{\infty} e \frac{\partial n_\mathrm{e}}{\partial t}\,\mathrm{d}x = \lim_{x \to \infty} e\psi_\mathrm{e}(x,t) \\ &= -\tilde{j}\,(t) = \frac{\mathrm{d}\tilde{Q}}{\mathrm{d}t}. \end{aligned} \tag{10}$$

The integral of $e n_\mathrm{i}(x)$ from any point $\bar{s}$ to $s(t)$ thus equals the charge $\tilde{Q}(t)$, up to a constant. There is exactly one $\bar{s}$ where that constant equals zero. This point is a convenient choice of the coordinate origin $x = 0$. It serves also as the origin of a second coordinate system, the charge coordinates $q = q(x)$, which are defined as

$$q(x) = \int_0^x e n_\mathrm{i}(x')\,\mathrm{d}x'. \tag{11}$$

The fluctuating sheath charge is then the charge coordinate of the electron sheath edge,

$$\tilde{Q}(t) = \int_0^{s(t)} e n_\mathrm{i}\,\mathrm{d}x = q(s(t)), \tag{12}$$

and the asymptotic condition for the electric field is

$$E(x,t) \underset{x \ll x_\mathrm{E}}{\longrightarrow} \frac{1}{\epsilon_0}(q(x) - \tilde{Q}(t)). \tag{13}$$

The advantage of these coordinate definitions is that the sheath can be analyzed without having to specify the electrode position x_E. This can be carried out as an *a posteriori* step. For the present research, the average sheath voltage is set equal to an applied voltage $\bar{V}$:

$$-\int_{x_\mathrm{E}}^{x_\mathrm{B}} \bar{E}(x)\,\mathrm{d}x \stackrel{!}{=} \bar{V}. \tag{14}$$

It may be assumed that this applied voltage is large enough so that the electron density at the electrode and left of it can be neglected. The full sheath charge $Q(t)$ can then be calculated as the sum of the fluctuating part $\tilde{Q}(t)$ and an additional constant $\bar{Q}$,

$$Q(t) = \int_{x_\mathrm{E}}^{\infty} e(n_\mathrm{i} - n_\mathrm{e})\,\mathrm{d}x = \bar{Q} + \tilde{Q}(t) = \int_{x_\mathrm{E}}^{s} e n_\mathrm{i}\,\mathrm{d}x. \tag{15}$$

The last identity shows that the electrode position is related to the phase-averaged sheath charge and the phase-avered electric field via

$$q(x_\mathrm{E}) = \int_0^{x_\mathrm{E}} e n_\mathrm{i}\,\mathrm{d}x = -\bar{Q} = \bar{E}(x_\mathrm{E}). \tag{16}$$

When the applied voltage is not sufficiently large, for example when the electrode is floating, the last two formulas cease to be exact. They remain, however, acceptable approximations: The ion current j_i and thus also the DC electron current $\bar{j}_\mathrm{e}$ are typically very small and can be considered as perturbations. For floating electrodes, this ansatz leads to the Hertz–Langmuir formula which provides an alternative possibility

for determining the electrode location x_E. For more details, see, for example, [16].

In the characteristic units introduced in section 1, the equations of the Electron Equilibrium Model can be simplified considerably. The input consists of the positive, continuous, and monotonically growing ion density $n_i(x)$ and of the average-free RF current $\tilde{j}(t)$ which is periodic in the scaled RF interval $[0, 2\pi]$. Two auxiliary integral quantities are defined: The charge coordinate $q(x)$ as the spatial integral of $n_i(x)$ from the origin to x,

$$q(x) = \int_0^x n_i(x')\,\mathrm{d}x', \tag{17}$$

$$\frac{\partial q}{\partial x} = n_i(x); \tag{18}$$

and the fluctuating sheath charge $\tilde{Q}(t)$ as the average-free temporal integral of $-\tilde{j}(t)$,

$$\tilde{Q}(t) = -\int_0^t \tilde{j}(t')\,\mathrm{d}t' + \int_0^{2\pi}\left(1 - \frac{t'}{2\pi}\right)\tilde{j}(t')\,\mathrm{d}t', \tag{19}$$

$$\frac{\mathrm{d}\tilde{Q}}{\mathrm{d}t} = -\tilde{j}(t). \tag{20}$$

The quantities to be determined are the electron density $n_e(x,t)$, the electron flux $\psi_e(x,t)$, and the electric field $E(x,t)$. They are governed by the equation of continuity, the relation of force equilibrium, Poisson's equation, and the current balance:

$$\frac{\partial n_e}{\partial t} + \frac{\partial \psi_e}{\partial x} = 0, \tag{21}$$

$$\epsilon^2\frac{\partial n_e}{\partial x} + E n_e = 0, \tag{22}$$

$$\frac{\partial E}{\partial x} = n_i - n_e, \tag{23}$$

$$-\psi_e + \frac{\partial E}{\partial t} = \tilde{j}(t). \tag{24}$$

The asymptotic conditions demand electron depletion and the field identity for $x \ll x_E$,

$$n_e(x,t) \underset{x\ll x_E}{\longrightarrow} 0, \tag{25}$$

$$E(x,t) \underset{x\ll x_E}{\longrightarrow} q(x) - \tilde{Q}(t), \tag{26}$$

and quasineutrality and a vanishing field for $x \gg x_B$,

$$n_e(x,t) \underset{x\gg x_B}{\longrightarrow} n_i(x), \tag{27}$$

$$E(x,t) \underset{x\gg x_B}{\longrightarrow} 0. \tag{28}$$

The displayed relations are not independent. To condense the Equilibrium Model further, the electron density n_e and the electron flux ψ_e are substituted as

$$n_e(x,t) = n_i(x) - \frac{\partial E}{\partial x} \equiv \frac{\partial}{\partial x}(q(x) - \tilde{Q}(t) - E(x,t)), \tag{29}$$

$$\psi_e(x,t) = -\tilde{j}(t) + \frac{\partial E}{\partial t} \equiv -\frac{\partial}{\partial t}(q(x) - \tilde{Q}(t) - E(x,t)). \tag{30}$$

Poisson's equation, the RF current balance, and the equation of continuity are then direct consequences and need not be postulated independently. The only remaining equation is the electron force balance. Expressed in terms of the electric field, the Equilibrium Model reads as follows, where the name $R_{\epsilon 0}$ is introduced for later use:

$$R_{\epsilon 0} := \epsilon^2\frac{\partial}{\partial x}\left(n_i - \frac{\partial E}{\partial x}\right) + E\left(n_i - \frac{\partial E}{\partial x}\right) = 0. \tag{31}$$

Also the asymptotic conditions of the model can be formulated in terms of the electric field. For the sheath limit $x \ll x_E$, the independent condition is

$$E(x,t) \underset{x\ll x_E}{\longrightarrow} q(x) - \tilde{Q}(t). \tag{32}$$

This implies asymptotic electron depletion and determines also the absolute location of the electron sheath edge $s(t)$ via the identity

$$q(s(t)) \overset{!}{=} \tilde{Q}(t). \tag{33}$$

In the plasma limit $x \gg x_B$, the asymptotic condition is that the electric field vanishes which implies asymptotic quasineutrality

$$E(x,t) \underset{x\gg x_B}{\longrightarrow} 0. \tag{34}$$

Finally, the electrode position is determined from the voltage drop condition

$$-\int_{x_E}^{x_B} \bar{E}(x)\,\mathrm{d}x \overset{!}{=} \bar{V}, \tag{35}$$

where the phase-averaged electric field is defined as

$$\bar{E}(x) = \frac{1}{2\pi}\int_0^{\pi} E(x,t)\,\mathrm{d}t. \tag{36}$$

The average sheath charge is then

$$\bar{Q} = -q(x_E). \tag{37}$$

3. Example ion dynamics and sheath model

To enable the construction of a realistic example, this section will outline a simple ion dynamics which can be solved alongside with the described Electron Equilibrium Model. Neclecting ionization and chemistry, the equation of continuity states that the ion flux ψ_i, i.e. the product of the ion density $n_i = n_i(x)$ and the ion velocity $v_i = v_i(x)$, is constant. The sign indicates that the flow is into the negative x-direction:

$$n_i v_i = -\psi_i = \text{const.} \tag{38}$$

The equation of motion describes the ion dynamics under the action of the phase-averaged electric field and collisional

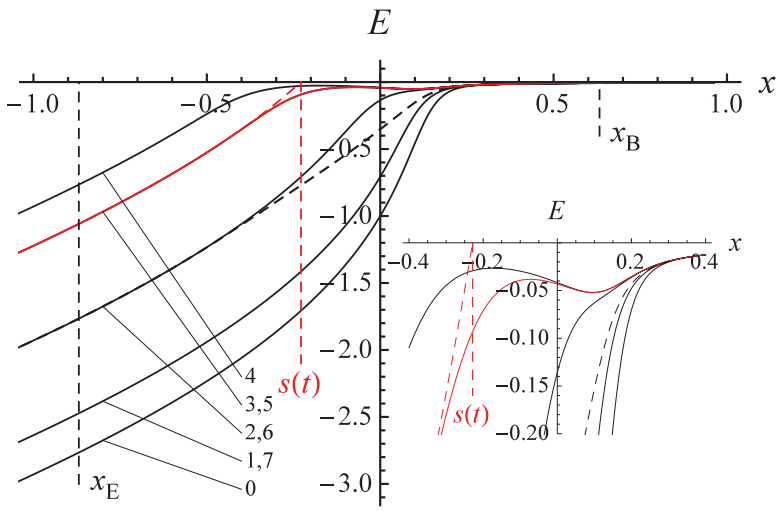

Figure 2. Phase-resolved electric field $E_{EQ}(x,t)$ in a sheath-plasma transition; conditions as in figure 1. The solid black lines show the field at $t_k = k\pi/4$, $k = 0..7$. Because of the symmetry $t \to 2\pi - t$, expansion and retraction curves coincide. The dashed black line is the time-averaged field $\bar{E}_{EQ}(x)$. The two red curves compare the Equilibrium Model (solid) to the Step Model (dashed) at $t_3 = 3\pi/4$. The inset enlarges the interval $[-0.4, 0.4]$ to resolve the transition to the ambipolar field.

friction with the neutral gas background. For the friction force, an effective model is chosen that combines the regimes of constant collision frequency ν_T/λ_i at low ion speed and constant mean free path λ_i at high speed [21]:

$$v_i \frac{\partial v_i}{\partial x} = \frac{e}{m_i}\bar{E} - \frac{1}{\lambda_i}\sqrt{v_T^2 + v_i^2}\; v_i. \tag{39}$$

The asymptotic condition of the ion model describes the assumption of transport equilibrium (validity of the drift regime) in the limit plasma $x \gg x_B$,

$$v_i(x) \underset{x\gg x_B}{\longrightarrow} \frac{e\lambda_i}{m_i \nu_T}\bar{E}(x). \tag{40}$$

In dimensionless notation, the equations of the ion model read

$$n_i v_i = -1, \tag{41}$$

$$v_i \frac{\partial v_i}{\partial x} = \bar{E} - \frac{1}{\lambda}\sqrt{u_T^2 + v_i^2}\; v_i, \tag{42}$$

$$v_i(x) \underset{x\gg x_B}{\longrightarrow} \frac{\lambda}{u_T}\bar{E}(x), \tag{43}$$

The combination of the Electron Equilibrium Model and the outlined ion model is already too complex to be solved analytically. A numerical solution, using the input from table 1, was found by discretizing the equations on the spatio-temporal domain $[x_E, x_B] \times [0, 2\pi]$ and solving the resulting algebra iteratively. The outcome is displayed in the following figures. Figure 1 shows the ion density $n_{i,EQ}(x)$ and the electron density $n_{e,EQ}(x,t)$ at different phases; figure 2 gives the corresponding electric field $E_{EQ}(x,t)$. Note the point $s(t)$ for a selected time t. One can clearly tell the space charge field left of $s(t)$ from the ambipolar field right of $s(t)$. Figure 3 shows the charge coordinate $q_{EQ}(x)$ in comparison with the ion density $n_{i,EQ}$.

4. Step model and advanced algebraic approximation

As discussed above, the difficulty to solve plasma models analytically motivates the search for suitable simplifications. Algebraic field models focus on the combination of the electron momentum balance and Poisson's equation. Early pioneers were Godyak [5] who introduced the so-called *Step Model (SM)* which approximates the rapid transition from electron depletion to quasineutrality as a sharp front at the sheath edge $s(t)$,

$$n_e(x,t) \approx \begin{cases} 0 & : \quad x < s(t) \\ n_i(x) & : \quad x > s(t) \end{cases}. \tag{44}$$

Substituted into Poisson's equation (23), this ansatz yields

$$\frac{\partial E}{\partial x} \approx \begin{cases} n_i(x) & : \quad x < s(t) \\ 0 & : \quad x > s(t) \end{cases}. \tag{45}$$

A straightforward integration then establishes an explicit formula for the electric field E_{SM}. Note the inherent problem: For $x > s(t)$, Poisson's equation is used to obtain E_{SM} as zero while it is actually the field itself that enforces quasineutrality:

$$E_{SM}(x,t) = \begin{cases} -\int_x^{s(t)} n_i(x')\,\mathrm{d}x \equiv q(x) - \tilde{Q}(t) & : \quad x < s(t) \\ 0 & : \quad x > s(t) \end{cases}. \tag{46}$$

An alternative derivation helps to assess the mathematical character of the approximation: Consider the condensed

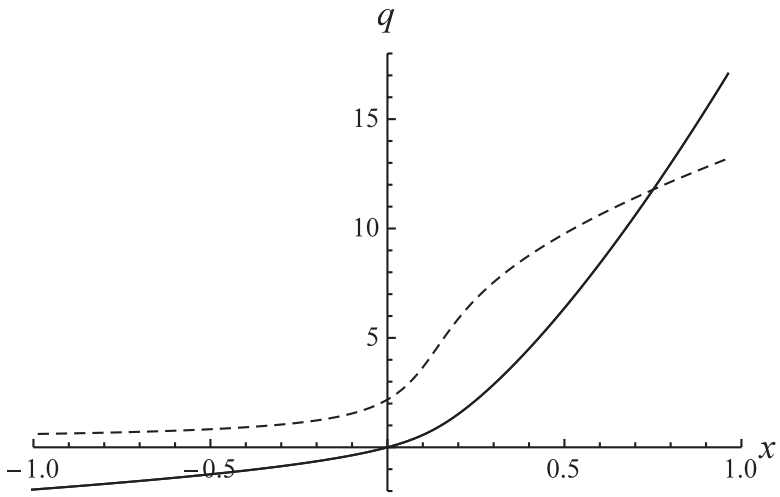

Figure 3. Solid: Charge coordinate function $q_{\mathrm{EQ}}(x)$, calculated with the Electron Equilibrium Model and the example ion model given in section IV. Dashed: Its derivative, the ion density $n_{\mathrm{i,EQ}}(x)$. (Divided by 2 to fit into the graph.) These functions are employed for all numerical examples.

formulation (31) of the Electron Equilibrium Model, here with the length ratio ϵ set equal to zero,

$$R_{00} := E\left(n_{\mathrm{i}} - \frac{\partial E}{\partial x}\right) = 0. \tag{47}$$

Clearly, either the electric field E itself is zero, or its derivative is equal to the ion density. Nontrivial solutions of equation (47) have the form (46), which thus can be characterized as the leading order of an expansion of the electrical field $E_{\mathrm{EQ}}(x,t)$ in the smallness parameter ϵ. Consequently, the Step Model accounts for the strong depletion field in the sheath (order ϵ^0) but misses the weak ambipolar field in the plasma (order ϵ^2). (In figure 2, the solid red curve represents the Equilibrium Model at a selected t; the dashed red curve gives the Step Model.) Considering also the equilibrium character of the model approximated, one can summarize: The Step Model E_{SM} represents the electric field in a plasma sheath transition when all thermal (finite ϵ) or dynamic (finite η) effects are neglected entirely.

In order to amend the Step Model, this author gave a solution of the Boltzmann–Poisson problem (22) and (23) that holds to order ϵ^2 [15]. It yields the space charge field for $x \ll s(t)$, the ambipolar field for $x \gg s(t)$, and a smooth interpolation in the transition region $x \approx s(t)$. In abbreviated notation (the transition terms are actually quite complicated):

$$E(x,t) = \begin{cases} -\displaystyle\int_x^{s(t)} n_{\mathrm{i}}(x')\,\mathrm{d}x & : \quad x < s(t) \\ -\epsilon^2 \dfrac{1}{n_{\mathrm{i}}}\dfrac{\partial n_{\mathrm{i}}}{\partial x} & : \quad x > s(t) \end{cases}$$
$$+ \quad \text{Transition terms in } \epsilon \text{ and } \epsilon^2 + O(\epsilon^3). \tag{48}$$

To render the model more applicable, a subsequent study carried out further simplifications while keeping the error $O(\epsilon^3)$ [16]. The resulting *Advanced Algebraic Approximation (AAA)* represents the electric field of a plasma sheath transition by

$$E_{\mathrm{AAA}}(x,t) = -\epsilon\sqrt{n_{\mathrm{i}}}\;\Xi_{\mathrm{S}}\left(\frac{q-\tilde{Q}}{\epsilon\sqrt{n_{\mathrm{i}}}}\right) - \epsilon^2 \frac{1}{n_{\mathrm{i}}}\frac{\partial n_{\mathrm{i}}}{\partial x}\;\Xi_{\mathrm{A}}\left(\frac{q-\tilde{Q}}{\epsilon\sqrt{n_{\mathrm{i}}}}\right). \tag{49}$$

Here, $\Xi_{\mathrm{S}}(\xi)$ and $\Xi_{\mathrm{A}}(\xi)$ are smooth (in fact analytical) 'switch functions', displayed in figure 4 and briefly reviewed in appendix A. They control the transition from the space charge field to the ambipolar field in dependence of their argument ξ which measures (in units of the Debye length) the relative distance of a point x from the electron sheath edge $s(t)$,

$$\xi = \frac{q(x) - \tilde{Q}(t)}{\epsilon\sqrt{n_{\mathrm{i}}(x)}} \approx \frac{x - s(t)}{\lambda_{\mathrm{D}}(s(t))}. \tag{50}$$

The original construction of the AAA in publications [15] and [16] was rather laborious. However, an *a posteriori* justification can easily be given. Starting point is again the formulation (31) of the Electron Equilibrium Model,

$$R_{\epsilon 0} := E\left(n_{\mathrm{i}} - \frac{\partial E}{\partial x}\right) + \epsilon^2 \frac{\partial}{\partial x}\left(n_{\mathrm{i}} - \frac{\partial E}{\partial x}\right) = 0, \tag{51}$$

with asymptotic conditions now expanded up to order ϵ^2,

$$E(x,t) \to \begin{cases} q(x) - \tilde{Q}(t) & : \quad x \ll x_{\mathrm{E}} \\ -\epsilon^2 \dfrac{1}{n_{\mathrm{i}}}\dfrac{\partial n_{\mathrm{i}}}{\partial x} & : \quad x \gg x_{\mathrm{B}} \end{cases}. \tag{52}$$

Ansatz (49) meets the asymptotic conditions (52) if the switch functions obey

$$\Xi_{\mathrm{S}}(\xi) \to \begin{cases} -\xi & : \quad \xi \ll 0 \\ 0 & : \quad \xi \gg 0 \end{cases}. \tag{53}$$

$$\Xi_{\mathrm{A}}(\xi) \to \begin{cases} 0 & : \quad \xi \ll 0 \\ 1 & : \quad \xi \gg 0 \end{cases}. \tag{54}$$

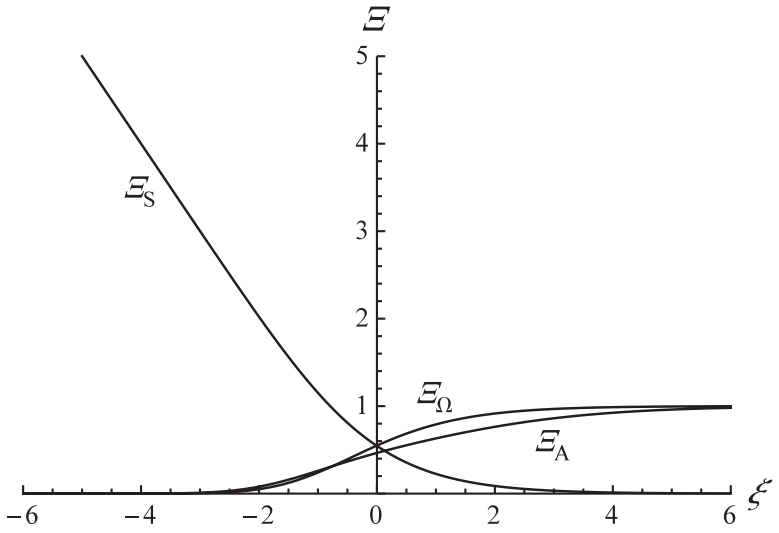

Figure 4. Analytic switch functions Ξ_S, Ξ_A, and Ξ_Ω in dependence of their argument $\xi \approx (x - s)/\lambda_D$. For an extended discussion of the switch functions and their derivation, see [15] and [16].

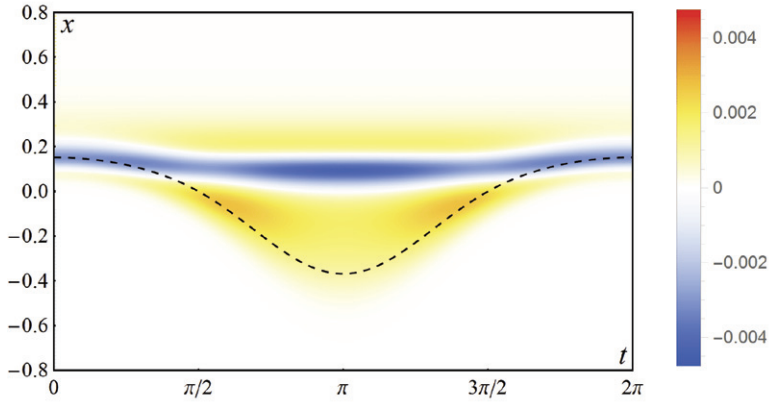

Figure 5. Phase-resolved deviation of the field of the Advanced Algebraic Approximation $E_{AAA}(x, t)$ from the numerically obtained field of the Equilibrium Model $E_{EQ}(x, t)$. The AAA is asymptotically exact with respect to the EQ field both in the sheath limit $x \ll x_E$ and the plasma limit $x \gg x_B$. The deviation is confined to the transition zone; it is maximal at $x \approx 0.1$ where the scaled curvature of the ion density $n_{i,EQ}(x)$ reaches its maximum. The maximal absolute deviation is about 0.0044, the maximal relative deviation about 8.5%.

In addition, the differential equation must be met as far as possible. Substituting ansatz (49), eliminating $q(x)$ in favor of ξ, and employing a series expansion with respect to ϵ yields

$$R_{\epsilon 0} = \epsilon R_S(\xi) n_i^{3/2} + \epsilon^2 R_A(\xi) \frac{\partial n_i}{\partial x} + O(\epsilon^3). \tag{55}$$

The residual $R_{\epsilon 0}$ can thus be made to vanish up to quadratic order in ϵ when the two functions $R_S(\xi)$ and $R_A(\xi)$ are identically zero. They are combinations of the switch functions and their first and second derivatives and read explicitly

$$R_S(\xi) = \frac{\partial^2 \Xi_S}{\partial \xi^2} - \Xi_S \left(\frac{\partial \Xi_S}{\partial \xi} + 1 \right), \tag{56}$$

$$R_A(\xi) = \Xi_S \left(\frac{1}{2} \xi \frac{\partial \Xi_S}{\partial \xi} - \frac{\partial \Xi_A}{\partial \xi} \right) - \left(\xi \frac{\partial^2 \Xi_S}{\partial \xi^2} + \Xi_A \left(\frac{\partial \Xi_S}{\partial \xi} + 1 \right) - \frac{\partial \Xi_S}{\partial \xi} - \frac{\partial^2 \Xi_A}{\partial \xi^2} - 1 \right) - \frac{1}{2} \Xi_S^2. \tag{57}$$

It can be shown that the switch functions $\Xi_S(\xi)$ and $\Xi_A(\xi)$ as defined in [16], shown in figure 4, and reviewed in appendix A, are unique in (i) rendering the residuals $R_S(\xi)$ and $R_A(\xi)$ zero and (ii) obeying the asymptotic conditions. The AAA thus obeys the differential equation (31) up to quadratic order in ϵ and shows correct asymptotic behavior, i.e. becomes equal to the space charge field for $x \ll s(t)$ and equal to the ambipolar field for $x \gg s(t)$. In summary: The Advanced Algebraic Approximation E_{AAA} represents the electric field in a plasma sheath transition with thermal effects up to quadratic order in $\epsilon = \lambda_D/l$. Dynamic effects, however, are not included; the parameter $\eta = \omega_{RF}/\omega_{pe}$ is set equal to zero.

It is instructive to subject the AAA to a numerical test. To facilitate a direct comparison, all parameters—ϵ, $n_i(x)$, $q(x)$, and $\tilde{Q}(t)$—are taken from the numerical solution EQ above.

In all respects, the deviations between the Equilibrium Model and the AAA field are small. In fact, on the scale of figure 2, the curves would be indistinguishable; their absolute difference is smaller than the line width. For that reason, figure 5 depicts the absolute deviation of the

models in the domain $[-0.8, 0.8] \times [0, 2\pi]$, defined as $\Delta E_{\mathrm{AAA}}(x,t) := E_{\mathrm{AAA}}(x,t) - E_{\mathrm{EQ}}(x,t)$. As the field representations agree asymptotically for $x \ll x_{\mathrm{E}}$ and $x \gg x_{\mathrm{B}}$, all deviations are confined to the transition zone. Furthermore, they are only present in those regions of the solution domain where the electron density does not vanish. (Compare the curve $x = s(t)$.)

The maximal deviation is located at $x \approx 0.1$ and $t = \pi$, i.e. deep in the quasineutral zone. It is thus the classical expression for the ambipolar field, $E_{\mathrm{A}} = -\epsilon^2 \frac{\partial n_{\mathrm{i}}}{\partial x}/n_{\mathrm{i}}$, that is primarily responsible for the error of the AAA. The point $x \approx 0.1$ corresponds to the maximum of the scaled curvature of the ion density which is the leading term of the residual.

5. Dynamic electron model

The reviewed AAA provides an asymptotically exact representation of the space charge and the ambipolar fields and a good interpolation in between. To describe electron heating, however, the formula does not yet suffice, as dynamic and dissipative fields are not included. Also the problematic assumption of a constant electron temperature must be dropped [2, 10]. For the plasma, where quasineutrality holds, a more general representation of the electric field is well-known as the generalized Ohm's law (including the ambipolar field):

$$E(x,t) = \frac{m_{\mathrm{e}}}{e^2 n_{\mathrm{i}}} \frac{\partial \tilde{j}}{\partial t} + \frac{\nu_{\mathrm{ce}} m_{\mathrm{e}}}{e^2 n_{\mathrm{i}}} \tilde{j} - \frac{m_{\mathrm{e}}}{e^3 n_{\mathrm{i}}} \frac{\partial}{\partial x}\left(\frac{\tilde{j}^2}{n_{\mathrm{i}}}\right) - \frac{1}{e n_{\mathrm{i}}} \frac{\partial}{\partial x}(n_{\mathrm{i}} T_{\mathrm{e}}). \tag{58}$$

The first two terms apply already for a homogeneous plasma; they represent the field which balances electron acceleration and momentum loss due to collisions with the background. The third term reflects the advective acceleration of the electrons by local density gradients. The fourth term balances the spatially and temporally varying electron pressure.

The derivation of an amended algebraic field model starts from a more general fluid model that includes dynamic and dissipative effects. The active variables in the *Dynamic Electron Model (DYN)* are the electron number density $n_{\mathrm{e}}(x,t)$ and the electron flux density $\psi_{\mathrm{e}}(x,t)$.

(Again, the ions are not dynamic but described by a temporally constant ion density $n_{\mathrm{i}}(x)$: When the radio frequency ω_{RF} is comparable to ω_{pe}, then it is surely much larger than ω_{pi}.) The solution domain is $[x_{\mathrm{E}}, x_{\mathrm{B}}]$, again extended to the full real axis via the virtual regions. Periodicity is assumed with respect to the fundamental RF period $[0,T]$, with $T = 2\pi/\omega_{\mathrm{RF}}$. The considered equations are the electron equation of continuity with ionization and attachment neglected as relatively slow processes,

$$\frac{\partial n_{\mathrm{e}}}{\partial t} + \frac{\partial \psi_{\mathrm{e}}}{\partial x} = 0, \tag{59}$$

and the electron equation of motion (dynamic momentum balance), where acceleration by the electric field and friction by collisional interaction with the background are accounted for. To close the model, the spatially and temporally varying electron temperature $T_{\mathrm{e}} = T_{\mathrm{e}}(x,t)$ is assumed as given or otherwise calculated (by an electron energy balance),

$$\frac{\partial}{\partial t}(m_{\mathrm{e}} \psi_{\mathrm{e}}) + \frac{\partial}{\partial x}\left(m_{\mathrm{e}} \frac{\psi_{\mathrm{e}}^2}{n_{\mathrm{e}}} + n_{\mathrm{e}} T_{\mathrm{e}}\right) = -e n_{\mathrm{e}} E - \nu_{\mathrm{ce}} m_{\mathrm{e}} \psi_{\mathrm{e}}. \tag{60}$$

Finally, the electric field and the charge density are coupled by Poisson's equation,

$$\epsilon_0 \frac{\partial E}{\partial x} = e(n_{\mathrm{i}} - n_{\mathrm{e}}). \tag{61}$$

As in the Equilibrium Model, the RF current density $\tilde{j}(t)$, the sum of the electron current and the displacement current, is spatially constant. It is taken as a periodic, average-free, given quantity, the control parameter of the model,

$$\tilde{j}(t) = -e\psi_{\mathrm{e}} + \epsilon_0 \frac{\partial E}{\partial t}, \tag{62}$$

with the fluctating sheath charge calculated as

$$\tilde{Q}(t) = -\int_0^t j(t')\,\mathrm{d}t' + \int_0^T \left(1 - \frac{t'}{T}\right) j(t')\,\mathrm{d}t'. \tag{63}$$

Again, sheath-like solutions of the model are sought. Electron depletion holds for $x \ll x_{\mathrm{E}}$; the electron density n_{e}, the electron flux density ψ_{e}, and the electric field E fulfill

$$n_{\mathrm{e}}(x,t) \underset{x \ll x_{\mathrm{E}}}{\longrightarrow} 0, \tag{64}$$

$$\psi_{\mathrm{e}}(x,t) \underset{x \ll x_{\mathrm{E}}}{\longrightarrow} 0, \tag{65}$$

$$\epsilon_0 \frac{\partial E}{\partial x} \underset{x \ll x_{\mathrm{E}}}{\longrightarrow} e n_{\mathrm{i}}, \tag{66}$$

$$\epsilon_0 \frac{\partial E}{\partial t} \underset{x \ll x_{\mathrm{E}}}{\longrightarrow} \tilde{j}(t). \tag{67}$$

For $x \gg x_{\mathrm{B}}$, the plasma is quasineutral; the electrons carry the full electric RF current $\tilde{j}$, and the electrical field is represented by the generalized Ohm's law,

$$n_{\mathrm{e}}(x,t) \underset{x \gg x_{\mathrm{B}}}{\longrightarrow} n_{\mathrm{i}}(x), \tag{68}$$

$$\psi_{\mathrm{e}}(x,t) \underset{x \gg x_{\mathrm{B}}}{\longrightarrow} -\tilde{j}(t)/e, \tag{69}$$

$$E(x,t) \underset{x \gg x_{\mathrm{B}}}{\longrightarrow} \frac{m_{\mathrm{e}}}{e^2 n_{\mathrm{i}}} \frac{\partial \tilde{j}}{\partial t} + \frac{m_{\mathrm{e}} \nu_{\mathrm{ce}}}{e^2 n_{\mathrm{i}}} \tilde{j} - \frac{m_{\mathrm{e}}}{e^3 n_{\mathrm{i}}} \frac{\partial}{\partial x}\left(\frac{\tilde{j}^2}{n_{\mathrm{i}}}\right) - \frac{1}{e n_{\mathrm{i}}} \frac{\partial}{\partial x}(n_{\mathrm{i}} T_{\mathrm{e}}). \tag{70}$$

The Dynamic Electron Model shares the equation of continuity and Poisson's equation with the Equilibrium Model. This allows to transfer the definitions of the axis origin $x = 0$

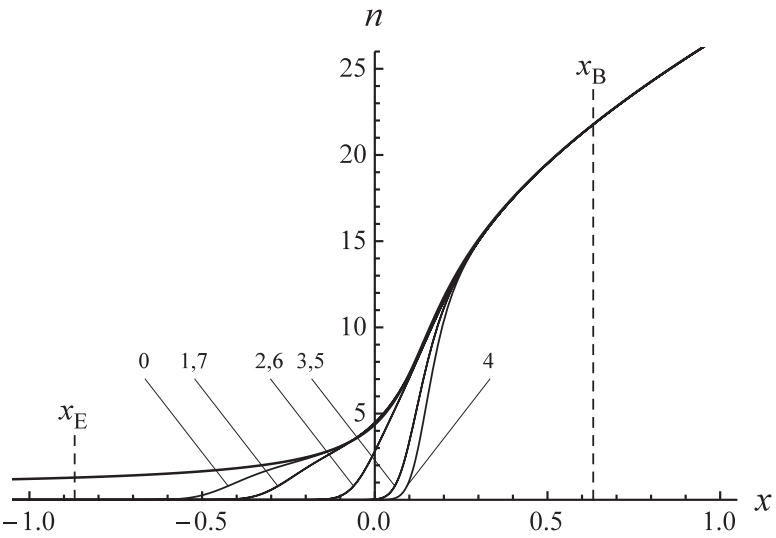

Figure 6. Electron density $n_{e,DYN}(x,t)$ (thin) in an RF modulated sheath-plasma transition at times $t_k = k\pi/4$, $k = 0..7$, obtained by the Dynamic Electron Model for the data set of example II. (The ion density $n_{i,EQ}(x)$ (thick) was taken from the Electron Equilibrium Model, compare figure 1.) The difference to the Electron Equilibrium Model is rather small, $\left|n_{e,DYN}(x,t) - n_{e,EQ}(x,t)\right| \lesssim 0.15$. Note, however, that the symmetry $t \to 2\pi - t$ is no longer exact.

and of the quantities $s(t)$ and $q(x)$. Integrating Poisson's equation, the asymptotic conditions of the electrical field for $x \ll x_E$ can then be expressed as

$$E(x,t) \underset{x \ll x_E}{\longrightarrow} \frac{1}{\epsilon_0}(q(x) - \tilde{Q}(t)). \tag{71}$$

Furthermore, Poisson's equation, the current relation, and the continuity equation can be solved for the electron density and flux,

$$n_e(x,t) = n_i - \frac{\epsilon_0}{e}\frac{\partial E}{\partial x}, \tag{72}$$

$$\psi_e(x,t) = \frac{\epsilon_0}{e}\frac{\partial E}{\partial t} - \frac{1}{e}\tilde{j}. \tag{73}$$

The remaining electron equation of motion becomes a partial differential equation for E, the dynamic analogon of the equilibrium (47). Expressed in the units defined in section II, the *Dynamic Electron Model (DYN)* does not only contain the spatial smallness parameter ϵ, but in addition also the temporal smallness parameter η. Moreover, it contains the scaled electron temperature that may be any periodic function $T_e(x,t)$ of order unity:

$$\begin{aligned} R_{\epsilon\eta} := {} & E\left(n_i - \frac{\partial E}{\partial x}\right) + \epsilon^2 \frac{\partial}{\partial x}\left(\left(n_i - \frac{\partial E}{\partial x}\right)T_e\right) \\ & + \eta^2\left(\frac{\partial}{\partial x}\left(\left(\frac{\partial E}{\partial t} - \tilde{j}\right)^2 \Big/ \left(n_i - \frac{\partial E}{\partial x}\right)\right) + \left(\frac{\partial^2 E}{\partial t^2} - \frac{\partial \tilde{j}}{\partial t}\right)\right. \\ & \left. + \nu\left(\frac{\partial E}{\partial t} - \tilde{j}\right)\right) = 0. \end{aligned} \tag{74}$$

The asymptotic conditions of the Dynamic Electron Model are

$$E(x,t) \to \begin{cases} q(x) - \tilde{Q}(t) & : \quad x \ll x_E \\ -\epsilon^2 \dfrac{1}{n_i}\dfrac{\partial}{\partial x}(n_i T_e) & : \quad x \gg x_B \\ +\eta^2 \dfrac{1}{n_i}\left(\dfrac{\partial \tilde{j}}{\partial t} + \nu\tilde{j} - \dfrac{\partial}{\partial x}\left(\dfrac{\tilde{j}^2}{n_i}\right)\right) & \end{cases}. \tag{75}$$

For a numerical example, the input of the equilibrium solution EQ given above was used, particularly the constant electron temperature (which is unity in the problem-adapted units). The solution domain was discretized with up to 1000 spatial and 128 temporal grid points. For the spatial discretization, co-moving charge coordinates $w(x,t) = q(x) - \tilde{Q}(t)$ were used, allowing for a refined resolution of the electron edge at $w = 0$. The temporal discretization was chosen equidistant. The resulting system of coupled nonlinear equations was solved by a damped Newton method. The overall relative error was uniformly below 10^{-6}.

With respect to the frequency ratio η, an comprehensive parameter study was conducted. For $\eta = 0$, the Equilibrium Model was recovered. At the value of example I, $\eta = 5.54 \times 10^{-2}$, the deviations were still very small. At the five times larger value of example II, $\eta = 0.277$, the dynamic effects were more pronounced. Figure 6 shows the electron densites $n_{e,DYN}(x,t)$ for selected time points t. The overall structure is similar to that of the Equilibrium Model: charge depletion to the left, quasineutrality to the right. The absolute deviation is small and becomes visible only in the inset of where the difference $n_{e,DYN}(x,t) - n_{e,EQ}(x,t)$ is depicted. Figure 7 shows the corresponding electrical field $E_{DYN}(x,t)$. Also here, the absolute deviation from $E_{EQ}(x,t)$ is small and can hardly be detected in the large figures. The inset, however, which displays the field difference between retraction

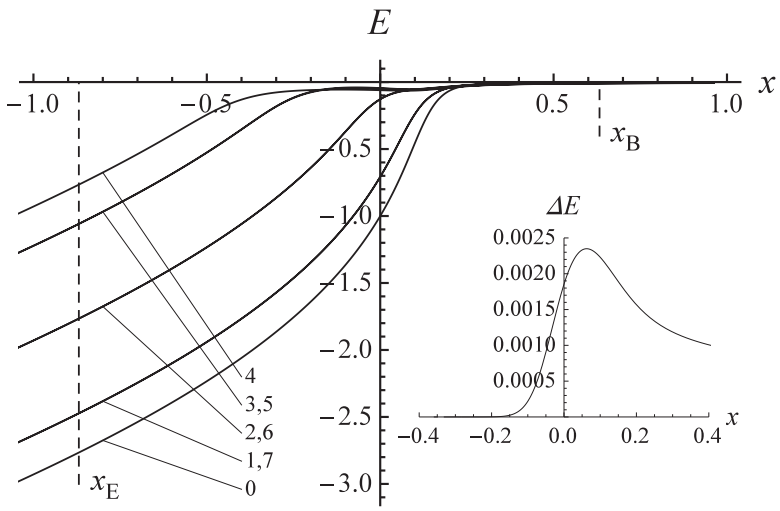

Figure 7. Electric field $E_{\mathrm{DYN}}(x,t)$ in an RF modulated sheath-plasma transition at $t_k = k\pi/4$, $k = 0..7$, obtained by the Dynamic Electron Model. Note that the symmetry $t \to 2\pi - t$ is no longer exact. The field difference ΔE between the retraction time $t_6 = 3\pi/2$ and the expansion time $t_2 = \frac{1}{2}\pi$ (inset) shows the influence of the generalized Ohmic field in the plasma.

and expansion, demonstrates that in the quasineutral zone the symmetry $t - 2\pi - t$ does no longer hold.

6. Smooth step model

The Dynamic Model (73) and (74) directly extends the Equilibrium Model (51) and (52). This suggests to generalize approximation (84) as well. Assuming the parameters ϵ and η as small and of the same order, an extended AAA—to be called the *Smooth Step Model (SSM)*—is sought which is correct up to quadratic order. Given the additive nature of (73) and (74), the following ansatz with a third term (where Ω stands for 'Ohmic') appears promising. Note that the possibility of a spatially and temporally varying electron temperature $T_e(x,t)$ is taken into account by replacing ϵ with $\epsilon\sqrt{T_e(x,t)}$:

$$E_{\mathrm{SSM}}(x,t) = -\epsilon\sqrt{n_i T_e}\;\Xi_S\left(\frac{q-\tilde{Q}}{\epsilon\sqrt{n_i T_e}}\right) - \epsilon^2\frac{1}{n_i}\frac{\partial}{\partial x}(n_i T_e)\;\Xi_A\left(\frac{q-\tilde{Q}}{\epsilon\sqrt{n_i T_e}}\right) + \eta^2\frac{1}{n_i}\left(\frac{\partial\tilde{j}}{\partial t} + \nu\tilde{j} - \frac{\partial}{\partial x}\left(\frac{\tilde{j}^2}{n_i}\right)\right)\Xi_\Omega\left(\frac{q-\tilde{Q}}{\epsilon\sqrt{n_i T_e}}\right). \quad (76)$$

Substituting this ansatz into (73), one obtains the following residual, where $O((\epsilon,\eta)^3)$ stands for terms cubic or higher in any combination of ϵ or η,

$$R_{\epsilon\eta} = \epsilon R_S(\xi) n_i^{3/2} T_e^{1/2} + \epsilon^2 R_A(\xi)\frac{\partial}{\partial x}(n_i T_e) + \eta^2 R_\Omega(\xi)\left(\frac{\partial\tilde{j}}{\partial t} + \nu\tilde{j} - \frac{\partial}{\partial x}\left(\frac{\tilde{j}^2}{n_i}\right)\right) + O((\epsilon,\eta)^3), \quad (77)$$

and the stretched spatial coordinate ξ is given by

$$\xi = \frac{q(x) - \tilde{Q}(t)}{\epsilon\sqrt{n_i(x)T_e(x,t)}} \approx \frac{x - s(t)}{\lambda_D(x)}. \quad (78)$$

$R_S(\xi)$ and $R_A(\xi)$ are defined as above and are identical to zero for the given $\Xi_S(\xi)$ and $\Xi_A(\xi)$. The additional residual function $R_\Omega(\xi)$ is defined as

$$R_\Omega(\xi) = \frac{\partial^2\Xi_\Omega}{\partial\xi^2} - \Xi_S\frac{\partial\Xi_\Omega}{\partial\xi} - \Xi_\Omega\left(\frac{\partial\Xi_S}{\partial\xi} + 1\right) - \frac{\partial\Xi_S}{\partial\xi} - 1. \quad (79)$$

The condition that $R_\Omega(\xi)$ vanishes identically provides a differential equation for the third switch function $\Xi_\Omega(\xi)$ that governs the Ohmic field. Its asymptotic conditions are

$$\Xi_\Omega(\xi) \to \begin{cases} 0 & : \quad \xi \ll 0 \\ 1 & : \quad \xi \gg 0 \end{cases}. \quad (80)$$

Also for this function, it can be shown that the explicit representation given in appendix A and shown in figure 4 is unique.

With these definitions, $E_{\mathrm{SSM}}(x,t)$ is a uniformly valid representation of the electric field in the extended solution domain $(-\infty,\infty)$. It is physically plausible, as it yields (i) the space charge field in the electron depleted sheath, (ii) the generalized Ohmic and ambipolar field in the quasineutral plasma, and (iii) a smooth interpolation for the transition in between. However, it must be emphasized that it is only an approximate solution of the Dynamic Electron Model (73) and (74): it was derived for the regime $\epsilon \ll 1$ and $\eta \ll 1$ and is correct only up to quadratic order in these smallness parameters.

To assess its performance, the SSM was evaluated with the same input as the model DYN. (Example II with ion density $n_{i,\mathrm{EQ}}(x)$.) The resulting $E_{\mathrm{SSM}}(x,t)$ is indeed close to $E_{\mathrm{DYN}}(x,t)$. In the scale of figure 7 the curves would be identical. Figure 8 shows the spatially and temporally resolved error $\Delta E_{\mathrm{SSM}}(x,t) = E_{\mathrm{SSM}}(x,t) - E_{\mathrm{DYN}}(x,t)$ in the domain $[-0.8, 0.8] \times [0, 2\pi]$. There are clearly two very different contributions:

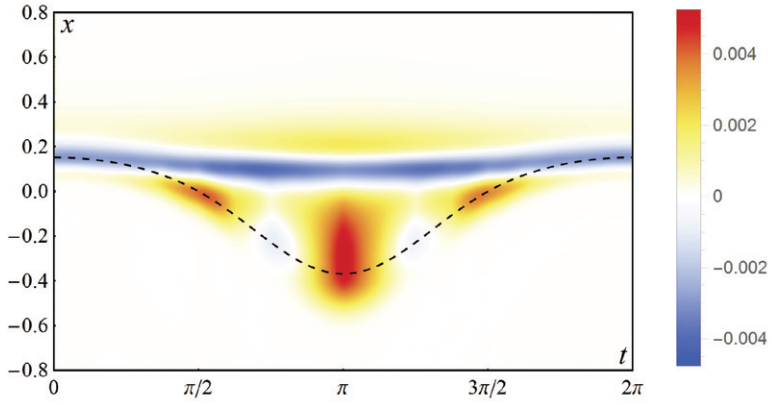

Figure 8. Spatially and temporally resolved deviation of the Smooth Step Model $E_{\mathrm{SSM}}(x,t)$ from the Dynamic Electron Model $E_{\mathrm{DYN}}(x,t)$, for the ion density $n_{\mathrm{i,EQ}}(x)$ and the data set of example II. E_{SSM} coincides with E_{DYN} both in the sheath limit $x \ll x_{\mathrm{E}}$ (where it gives the space charge field) and in the plasma limit $x \gg x_{\mathrm{B}}$ (where it reduces to the generalized Ohmic field). The error appears only in the transition region: The static error, inherited from the AAA, is maximal at $x \approx 0.1$ where the ion density has a large scaled curvature. The dynamic error is located between $x \approx -0.5$ and $x \approx -0.2$ where plasma oscillations during sheath collapse are present in E_{DYN} but not in E_{SSM}. The maximal absolute deviation is about 0.0048, the maximal relative deviation about 9.6%.

- The 'static' deviation at $x \approx 0.1$ is directly inherited from the AAA, compare figure 5. It is caused by the ambipolar field term which becomes inaccurate when the scaled gradient or curvature of the ion density become too large. These quantities, however, are determined by the solution itself. Numerical studies have shown that they depend only weakly of the details of the ion dynamics, particularly the level of collisionality. The given example is typical: The maximum of $\epsilon(x) = \left|\lambda_{\mathrm{D}} \frac{1}{n_{\mathrm{i}}} \frac{\partial n_{\mathrm{i}}}{\partial x}\right|$ is assumed at $x \approx 0.06$ and has a value of $\epsilon_{\max} = 0.22$; the scale of the relative error is $\epsilon_{\max}^2 \approx 0.05$.
- The 'dynamic' error in the interval $[-0.5, -0.2]$ arises from the fact that the SSM, in its character, is a *quasi-static* model. Dynamic effects are taken into account only in form of perturbative corrections: The SSM does not assume *exact* force equilibrium as the AAA but *approximate* force equilibrium. The differentials—the forces of inertia and friction—are given by terms of higher order in η. The Dynamic Electron Model, in contrast, contains also truly dynamic phenomena, namely plasma oscillations with frequency $\omega_{\mathrm{pe}} = \omega_{\mathrm{RF}}/\eta \sim 1/\eta$. These oscillations get excited when the frequency ratio ceases to be a small parameter. In the regime of example II, at $\eta = 0.277$, this begins to be the case and leads to deviations between E_{SSM} and E_{DYN} of about 10%.

In summary: If a 10% error is acceptable, the SSM can be applied to capacitively coupled RF plasmas of all levels of collisionality that meet the frequency condition $\omega_{\mathrm{RF}} \lesssim 0.25\,\omega_{\mathrm{pe}}$. This holds for most cases of practical interest. (The high frequency, low density discharges studied in [23], this Special Issue, however, represent counter examples.)

7. Summary and conclusions

It was the goal of this work to analyze the electric field in a capacitively coupled discharge, with particular emphasis on algebraic (closed) field models. In the course of the investigation, two previously defined algebraic field models were reviewed, the *Step Model (SM)* by Godyak [5] and the *Advanced Algebraic Approximation (AAA)* by this author [15, 16], and a new model was proposed, the *Smooth Step Model (SSM)*. Two underlying non-algebraic models acted as standards and were solved numerically, the *Electron Equilibrium Model (EQ)* and the *Dynamic Electron Model (DYN)*. How do the field models relate, what are their specific assumptions, and what are their respective areas of application? This chapter will discuss and summarize the results. (See also table 2.)

In principle, all three algebraic models assume the same regime, characterized by the smallness of the dimensionless numbers ϵ and η. The first smallness parameter ϵ is the ratio of the Debye length λ_{D} to the ion scale length l in the sheath; or, equivalently, the square root of the thermal voltage T_{e}/e to the voltage scale $\hat{V}$. It measures the relative influence of thermal effects and vanishes when the electron temperature T_{e} is set equal to zero,

$$\epsilon = \frac{\lambda_D}{l} \equiv \sqrt{\frac{T_{\mathrm{e}}}{e\hat{V}}} \equiv \sqrt{\frac{\epsilon_0 T_{\mathrm{e}}}{e^2 n_{\mathrm{i}}}} \frac{1}{n_{\mathrm{i}}} \frac{\partial n_{\mathrm{i}}}{\partial x}\bigg|_{\mathrm{typ}}. \tag{81}$$

Note that the parameter ϵ, in a way, is 'naturally small'. It assumes its maximum in a floating sheath where no modulation is present and the voltage scale $\hat{V}$ can be identified with the floating voltage V_{fl}. Typically, $V_{\mathrm{fl}} \approx 5T_e/e$ and thus

$$\epsilon \leq \epsilon_{\mathrm{fl}} = \sqrt{\frac{T_{\mathrm{e}}}{eV_{\mathrm{fl}}}} \approx 0.4. \tag{82}$$

The second smallness parameter η is the ratio of the applied radio frequency ω_{RF} or the collision frequency ν_{ce} to the sheath plasma frequency ω_{pe}. It measures the relative influence of dynamic effects and vanishes when the electron mass m_{e} is set equal to zero,

$$\eta = \frac{\omega_{\mathrm{RF}}}{\omega_{\mathrm{pe}}} \equiv \omega_{\mathrm{RF}} \sqrt{\frac{\epsilon_0 m_{\mathrm{e}}}{e^2 n_{\mathrm{i}}}}\bigg|_{\mathrm{typ}}. \tag{83}$$

Table 2. Assumptions of the field models described in this study.

		Thermal effects (finite electron temperature)		
		$\epsilon = 0$	$\epsilon \ll 1$	ϵ not restricted
Dynamic effects (finite electron mass)	$\eta = 0$	Step model (SM)	Advanced algebraic approximation (AAA)	Electron equilibrium model (EQ)
	$\eta \ll 1$	—	Smooth step model (SSM)	—
	η not restricted	—	—	Dynamic electron model (DYN)

Note: The Electron Equilibrium Model and the Dynamic Electron Model are standards; they were solved numerically for an example. The Step Model, the Advanced Algebraic Approximation, and the Smooth Step Model are algebraic field models that make different assumptions on the parameters ϵ and η.

To employ either of the three algebraic models, the ion density $n_i(x)$ and its spatial integral, the charge coordinate $q(x)$, must be known, likewise the fluctuating sheath charge $\tilde{Q}(t)$, which is found as the average-free time integral of the negative RF current density $\tilde{j}(t)$. (Alternatively, $\tilde{Q}(t)$ itself may be considered as the control parameter of the model.)

Of the three field models, the Step Model implements the assumptions most drastically: It neglects all thermal and dynamic effects completely and sets both ϵ and η equal to zero; either from the start, as in [5], or by taking the corresponding limits of the other models. Equivalently, both the electron temperature T_e and the electron mass m_e are set to equal zero. Translated back into physical units, the Step Model field reads

$$E_{SM}(x,t) = \begin{cases} \dfrac{1}{\epsilon_0}(q-\tilde{Q}) & : \quad q < \tilde{Q} \Leftrightarrow x < s(t) \\ = \dfrac{e}{\epsilon_0}\displaystyle\int_x^{s(t)} n_i(x')\,\mathrm{d}x' & \\ 0 & : \quad q > \tilde{Q} \Leftrightarrow x > s(t) \end{cases} . \tag{84}$$

The Step Model is thus the simplest algebraic field model, for the price that it only covers the strong space charge field in the depletion region $x \ll s(t)$ and neglects the weaker field contributions in the non-depleted zone $x \gtrsim s(t)$. It is thus applicable when the emphasis is on leading order sheath phenomena such as the overall charge-voltage relation $V = V(Q)$. Important examples are the sheath models by Lieberman and their generalizations [6–14]. Note that all these models require boundary conditions at the (problematic) 'sheath edge' because the Step Model fails to describe the field in the plasma. They also degenerate in cases where the applied RF voltage is smaller than the floating voltage.

The second model in this study, the *Advanced Algebraic Approximation*, implements only one of the assumptions drastically: Dynamic effects are neglected; the parameter η and the electron mass m_e are set equal to zero. The parameter ϵ is considered small but finite and thermal effects are kept up to quadratic order. In physical units, the AAA model is

$$E_{AAA}(x,t) = -\sqrt{\frac{n_i T_e}{\epsilon_0}}\,\Xi_S\left(\frac{q-\tilde{Q}}{\sqrt{\epsilon_0 n_i T_e}}\right) - \frac{1}{e n_i}\frac{\partial}{\partial x}(n_i T_e)\,\Xi_A\left(\frac{q-\tilde{Q}}{\sqrt{\epsilon_0 n_i T_e}}\right). \tag{85}$$

Comparison with the Step Model shows that the thermal effects enter in two different ways. First, they smoothen the sharp transition from the depletion zone to the quasineutral zone; the relevant scale being the Debye length λ_D. And second, they induce an additional term which contains the ambipolar field, the dominant field in the plasma. The AAA is thus useful for models which aim to describe not only the sheath, but also its transition into the plasma. Boundary conditions at the 'sheath edge' are no longer required. A recent study made use of this and focused on the question of a collisionally modified Bohm criterion [20].

Finally, the last field formula, newly derived in this study, is the *Smooth Step Model* (SSM) which covers thermal (finite electron temperature) *and* dynamic (finite electron mass) effects. This was achieved by assuming the parameters $\epsilon = \lambda_D/l$ and $\eta = \omega_{RF}/\omega_{pe}$ as small but finite, and carrying out a systematic expansion of the Dynamic Electron Model up to second order. As ϵ is naturally small, it is the second condition that is critical. Errors of 10%, as seen above, require $\omega_{RF} \lesssim 0.25\,\omega_{pe}$ which is met for most capacitively coupled RF discharges of interest. (This refers to the maximum of the local error; the averaged error is typically much smaller.) Translated back into physical units, the newly proposed Smooth Step Model reads

$$E_{SSM}(x,t) = -\sqrt{\frac{n_i T_e}{\epsilon_0}}\,\Xi_S\left(\frac{q-\tilde{Q}}{\sqrt{\epsilon_0 n_i T_e}}\right) - \frac{1}{e n_i}\frac{\partial}{\partial x}(n_i T_e)\,\Xi_A\left(\frac{q-\tilde{Q}}{\sqrt{\epsilon_0 n_i T_e}}\right) + \frac{m_e}{e^2 n_i}\left(\frac{\partial \tilde{j}}{\partial t} + \nu_{ce}\tilde{j} - \frac{1}{e}\frac{\partial}{\partial x}\left(\frac{\tilde{j}^2}{n_i}\right)\right)\Xi_\Omega\left(\frac{q-\tilde{Q}}{\sqrt{\epsilon_0 n_i T_e}}\right). \tag{86}$$

As desired, the Smooth Step Model establishes a physically transparent algebraic formula that gives (i) the space charge field in the electron-depleted sheath, (ii) the generalized Ohmic field in the quasineutral plasma, and (iii) a smooth interpolation for the transition in between. It accounts for thermal and dynamic effects, allows for a temporally and spatially structured electron temperature and is of high accuracy, provided that the frequency condition is met. It is ready to serve as a building block for theories on the subject of this Special Issue, electron heating in technical plasmas. Work in this direction is underway.

Acknowledgments

The author gratefully acknowledges support by Deutsche Forschungsgemeinschaft (DFG) via Research Group FOR 1123 *Physics of Microplasmas* and Sonderforschungsbereich SFB-TR 87 *Gepulste Hochleistungsplasmen zur Synthese nanostrukturierter Funktionsschichten*. He also thanks the members of the Institute for Theoretical Electrical Engineering and the Research Department *'Plasmas with Complex Interactions* for many interesting discussions, and the referees for their helpful comments.

Appendix A. The switch functions Ξ_S, Ξ_A, and Ξ_Ω

The three switch functions Ξ_S, Ξ_A, and Ξ_Ω employed in this manuscript can be viewed as special functions (in the same sense as sine or cosine). They are uniquely defined in terms of certain differential equations and asymptotic conditions. For the convenience of the reader, this appendix gives an overview, summarized from [15, 16], and a numerical table (table A1).

The formalism is motivated by the standard fluid theory of the transition from electron depletion to quasi-neutrality. Taking the ion density as a given, the starting point is the scaled Bolzmann–Poisson equation for the electric potential Φ,

$$-\frac{\partial^2\Phi}{\partial x^2} = n_i(x) - \exp\left(\frac{\Phi}{\epsilon^2}\right). \tag{A.1}$$

Here, the potential is measured in units of the sheath voltage (compare units of table 1), densities are measured in units of the ion density at the electron edge, moved to the origin, and lengths are measured in units of the ion gradient length. (Therefore, $n_i(0) = n_i'(0) = 1$.) The asymptotic boundary conditions are

$$\begin{aligned} \frac{\partial\Phi}{\partial x} &\to \int_x^0 n_i(x')dx' \quad : \quad x \ll 0 \\ \Phi(x) &\to \epsilon^2 \ln(n_i(x)) \quad : \quad x \gg 0 \end{aligned}. \tag{A.2}$$

Approximate solutions are sought which exploit the smallness of the ratio ϵ of the Debye length to the gradient length at the electron edge. Obviously, a consistent ansatz is

$$\Phi(x) = \epsilon^2\Psi_0(x/\epsilon) + \epsilon^3\Psi_1(x/\epsilon). \tag{A.3}$$

This proves sucessful up to quadratic order in ϵ, when the following equations and asymptotic boundary conditions hold, with the constants found as $d_0 = -1$ and $d_1 \approx 0.387652$:

$$-\frac{\partial^2\Psi_0}{\partial\xi^2} + \exp(\Psi_0) = 1, \tag{A.4}$$

$$\Psi_0 \to \begin{cases} d_0 - \frac{1}{2}\xi^2 & : \quad \xi \ll 0 \\ 0 & : \quad \xi \gg 0 \end{cases}, \tag{A.5}$$

Table A1. Numerical values of the switch functions Ξ_S, Ξ_A, and Ξ_Ω in the interval [− 6.0,19.0].

ξ	$\Xi_S(\xi)$	$\Xi_A(\xi)$	$\Xi_\Omega(\xi)$
− 6.0	6.000 000	0.000 000	0.000 000
− 5.5	5.500 000	0.000 001	0.000 000
− 5.0	5.000 000	0.000 007	0.000 001
− 4.5	4.500 003	0.000 063	0.000 015
− 4.0	4.000 029	0.000 440	0.000 123
− 3.5	3.500 215	0.002 370	0.000 805
− 3.0	3.001 245	0.009 846	0.004 088
− 2.5	2.505 731	0.031 659	0.016 193
− 2.0	2.021 057	0.079 494	0.050 179
− 1.5	1.562 388	0.158 766	0.122 726
− 1.0	1.151 580	0.260 383	0.241 283
− 0.5	0.809 236	0.366 574	0.392 686
0.0	0.545 081	0.464 784	0.549 122
0.5	0.354 969	0.552 264	0.685 729
1.0	0.225 535	0.630 699	0.791 092
1.5	0.140 896	0.701 205	0.865 642
2.0	0.087 051	0.763 476	0.915 456
2.5	0.053 405	0.816 813	0.947 541
3.0	0.032 620	0.860 977	0.967 734
3.5	0.019 870	0.896 400	0.980 262
4.0	0.012 083	0.924 031	0.987 966
4.5	0.007 340	0.945 074	0.992 678
5.0	0.004 456	0.960 779	0.995 550
5.5	0.002 705	0.972 298	0.997 298
6.0	0.001 641	0.980 623	0.998 360
6.5	0.000 996	0.986 563	0.999 005
7.0	0.000 604	0.990 753	0.999 396
7.5	0.000 366	0.993 681	0.999 634
8.0	0.000 222	0.995 709	0.999 778
8.5	0.000 135	0.997 102	0.999 865
9.0	0.000 082	0.998 053	0.999 918
9.5	0.000 050	0.998 698	0.999 950
10.0	0.000 030	0.999 133	0.999 970
10.5	0.000 018	0.999 425	0.999 982
11.0	0.000 011	0.999 620	0.999 989
11.5	0.000 007	0.999 750	0.999 993
12.0	0.000 004	0.999 836	0.999 996
12.5	0.000 002	0.999 893	0.999 998
13.0	0.000 001	0.999 930	0.999 999
13.5	0.000 001	0.999 954	0.999 999
14.0	0.000 001	0.999 970	0.999 999
14.5	0.000 000	0.999 981	1.000 000
15.0	0.000 000	0.999 988	1.000 000
15.5	0.000 000	0.999 992	1.000 000
16.0	0.000 000	0.999 995	1.000 000
16.5	0.000 000	0.999 997	1.000 000
17.0	0.000 000	0.999 998	1.000 000
17.5	0.000 000	0.999 999	1.000 000
18.0	0.000 000	0.999 999	1.000 000
18.5	0.000 000	0.999 999	1.000 000
19.0	0.000 000	1.000 000	1.000 000

Note: To the left and the right of the inverval, the asymptotic behavior applies.

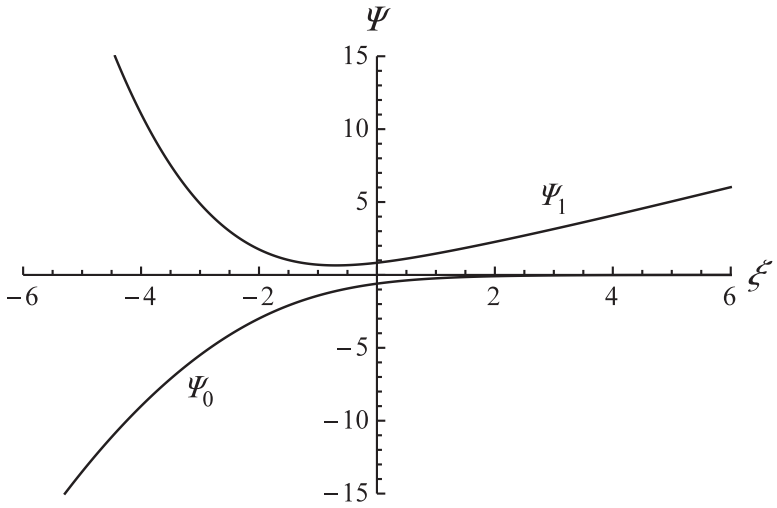

Figure A1. Basis functions Ψ_0 and Ψ_1 in dependence of their argument $\xi \approx (x - s)/\lambda_D$. For an extended discussion of the sheath functions and their derivation, see reference [15].

$$-\frac{\partial^2 \Psi_1}{\partial \xi^2} + \exp(\Psi_0)\Psi_1 = \xi, \tag{A.6}$$

$$\Psi_1 \to \begin{cases} d_1 - \dfrac{1}{6}\xi^3 & : \quad \xi \ll 0 \\ \xi & : \quad \xi \gg 0 \end{cases}. \tag{A.7}$$

The basis functions Ψ_0 and Ψ_1 are displayed in figure A1 in dependence of their argument ξ. In terms of them, the three switch functions Ξ_S, Ξ_A, and Ξ_Ω are then defined as follows; they render the residuals R_S, R_A, and R_Ω—equations (56), (57), and (78)—identically zero and fulfill the corresponding asymptotic conditions (53), (54), and (79):

$$\Xi_S(\xi) = \frac{\partial \Psi_0}{\partial \xi}, \tag{A.8}$$

$$\Xi_A(\xi) = \frac{\partial \Psi_1}{\partial \xi} - \frac{1}{2}\xi \frac{\partial \Psi_0}{\partial \xi}, \tag{A.9}$$

$$\Xi_\Omega(\xi) = \exp(\Psi_0(\xi)). \tag{A.10}$$

Arising from regular solutions of ordinary differential equations, the switch functions are smooth and analytical functions of their argument ξ. (Note the terminology change from [16], introduced to aid the memory: Ξ_S, responsible for the space charge field, was prior called Ξ_0; Ξ_A, governing the ambipolar field, was prior called Ξ_1, Ξ_Ω, controlling the generalized Ohmic field was prior called Σ_0 and played a different role.) Several numerical options exist to calculate the switch functions explicitly:

- The differential equations of the basis functions (A4)–(A7) can be solved numerically and the definitions (A8)–(A10) be applied.
- The differential equations of the switch functions themselves (56), (57), (78) with their asymptotic conditions (53), (54), (79) can be directly.
- Taylor series for the basis functions or the switch functions can be derived from the differential equations and numerically evaluated.

The author originally carried out the last program for the basis functions Ψ_0 and Ψ_1 and on that basis constructed numerical subroutines for the switch functions Ξ_S, Ξ_A, and Ξ_Ω. These routines are accurate up to errors of order 10^{-12}. For all practical purposes, however, this is much more than necessary. Table A1, when interpolated with cubic splines, gives an accuracy better than 10^{-4}; splines of order 7 result in accuracies better than 10^{-6}. Considering that the SSM has an error of a few percent, and that curves cannot be told apart when differing by less than a percent of the scale, this is entirely sufficient.

References

[1] Lieberman M A and Lichtenberg A J 2005 *Principles of Plasma Discharges and Materials Processing* 2nd edn (New York: Wiley)
[2] Schulze J, Donko Z, Derzsi A, Korolov I and Schuengel E 2015 *Plasma Sources Sci. Technol.* **24** 015019
[3] Lafleur T, Chabert P and Booth J P 2014 *Plasma Sources Sci. Technol.* **23** 035010
[4] Hemke T, Eremin D, Mussenbrock T, Derzsi A, Donko Z, Dittmann K, Meichsner J and Schulze J 2013 *Plasma Sources Sci. Technol.* **22** 015012
[5] Godyak V A 1976 *Fiz. Plasmy* **2** 141 (in Russian) Godyak V A 1976 *Sov. J. Plasma Phys.* **2** 78 (English Translation)
[6] Lieberman M A 1988 *IEEE Trans. Plasma Sci.* **16** 638
[7] Lieberman M A 1989 *IEEE Trans. Plasma Sci.* **17** 338
[8] Godyak V A and Sternberg N 1990 *Phys. Rev.* **42** 2299
[9] Sobolewski M A 2000 *Phys. Rev.* E **62** 8540
[10] Gozadinos G, Turner M M and Vender D 2001 *Phys. Rev. Lett.* **87** 135004

[11] Robiche J, Boyle P C, Turner M M and Ellingboe A R 2003 *J. Phys. D: Appl. Phys.* **36** 1810
[12] Boyle P C, Robiche J and Turner M M 2004 *J. Phys. D: Appl. Phys.* **37** 1451
[13] Xiang N and Waelbroeck F L 2004 *J. Appl. Phys.* **95** 860
[14] Rahman M T, Dewan M N A, Ahmed A and Chowdhury M R H 2013 *IEEE Trans. Plasma Sci.* **41** 17
[15] Brinkmann R P 2007 *J. Appl. Phys.* **102** 093303
[16] Brinkmann R P 2009 *J. Phys. D: Appl. Phys.* **42** 194009
[17] Kratzer M, Brinkmann R P, Sabish W and Schmidt H 2001 *J. Appl. Phys.* **90** 2169
[18] Schulze J, Donko Z, Heil B, Luggenhoelscher D, Mussenbrock T, Brinkmann R P and Czarnetzki U 2008 *J. Phys. D: Appl. Phys.* **41** 105214
[19] Heil B, Schulze J, Mussenbrock T, Brinkmann R P and Czarnetzki U 2008 *IEEE Trans. Plasma Sci.* **36** 1404
[20] Brinkmann R P 2011 *J. Phys. D: Appl. Phys.* **44** 042002
[21] Hornbeck J A 1951 *Phys. Rev.* **84** 615
[22] Salabas A and Brinkmann R P 2006 *Japan. J. Appl. Phys.* **45** 5203
[23] Wilczek S, Trieschmann J, Schulze J, Schuengel E, Brinkmann R P, Derzsi A, Korolov I, Donko Z and Mussenbrock T 2015 *Plasma Sources Sci. Technol.* **24** 024002